RSC Advances

ROYAL SOCIETY OF CHEMISTRY

www.rsc.org/advances

The pH-controlled Multiple-drug delivery by A Novel Antibacterial Nanocomposite for combination therapy

Fatemeh Bazmi zeynabad [1,2], Roya Salehi [3,4]*, Effat Alizadeh [4,5], Hossein Samadi Kafil [2], Azad Mohammad Hassanzadeh [2,5] and Mehrdad Mahkam[1]*

[1] Chemistry Department, Azarbaijan Shahid Madani University, Tabriz, Iran

[2] Drug Applied Research Center, Tabriz University of Medical Sciences, Tabriz, Iran

[3] Reseach Center for Pharmaceutical Nanotechnology, Tabriz University of Medical Sciences, Tabriz, Iran

[4] Faculty of Advanced Medical Science, Tabriz University of Medical Sciences, Tabriz, Iran

[5] Biotechnology Research Center, Tabriz University of Medical Sciences, Tabriz, Iran

Address for correspondence:
1 R. Salehi, Drug Applied Research Center, Tabriz University of medical sciences, Tabriz, Iran. Tel: +984113363161. Fax: +984113363132. Email: salehiro@tbzmed.ac.ir

2 M. Mahkam, Chemistry Department, Azarbaijan Shahid Madani University, Tabriz, Iran. Tel: +984124327500. Fax: +984124327500. Email: mahkam@azaruniv.edu

Abstract

Nanoparticle-based combination therapies have shown several unique features that are untenable in traditional chemotherapy. The present attempt is intended to prepare a novel smart multifunctional drug delivery system based on cationic silica based polymer-clay nanocomposites for combination cancer therapy. The intercalation of silica based copolymers into montmorillonite (MMT) was achieved through an ion exchange process. The structure of the resulting nanocomposites was characterized by means of XRD, FT-IR, TG-DTA and SEM. This nanocomposite was used for multiple drug delivery of two anticancer drugs doxorubicin (DOX) and methotrexate (MTX) and an antibacterial agent ciprofloxacin (CIP). The in vitro antimicrobial activity of nanocomposites and CIP loaded nanocomposites were tested in growth inhibition of *Escherichia coli* and *Pseudomonas aeruginosa* bacteria by MIC method. Furthermore, the potential antitumoral activity of this combined therapy system was evaluated against T47D cell lines by MTT assay and qRT-PCR. XRD results proved successful interaction of MMT with cationic silica based copolymer. The nanocomposites showed an encapsulation efficiency of about 95% for mentioned drugs. The cumulative in vitro release of the

DOX/MTX/CIP-loaded nanocomposites revealed that the individual drug can be controlled release with ability to distinguish between tumor tissues. Cell viability tests additional confirmed that the dual-administration of DOX with MTX had a higher cytotoxicity to the mentioned cells in comparison with free dual drug forms. The in vitro antimicrobial results revealed good antimicrobial activities of both blank nanocomposite and CIP loaded nanocomposite. Therefore, dual anticancer drug-loaded antibacterial smart nanocomposite has the potential to be used for combination cancer therapy.

Keywords: antibacterial polymers, combination therapy, dual anticancer drug, sustained release, stimuli responsive nanocomposite

1. Introduction

Montmorillonite (MMT) is a member of the smectite groups (M Parolo et al., 2011). It has a naturally occurring layered configuration made from silica tetrahedral sheets layered among alumina octahedral sheets at a ratio of 2:1, respectively. MMT have general formula- M^{+}_{x+y} (Al_{2-x}) $(OH)_2$ $(Si_{4-y}$ Aly) O_{10}, with a unit thickness of 1 nm or less with negative charge at the surface of the crystal that neutralized by cations (Na, Ca and occasionally K) are held at the interlayer spaces(M Datta and M Kaur, 2014, A Darehkordi et al., 2012). The cations in the interlaminar area of natural montmorillonite are responsible for the activity and substitution reactions with other inorganic and organic materials (PC Thomas et al., 2011, N Negrete-Herrera et al., 2006). MMT also contains dangling hydroxyl end-groups on the surfaces that can be exchanged with other ions (GV Joshi et al., 2009a). MMT has excellent properties such as, large specific surface area, colloidal particle size, high cation exchange and swelling capacity, adhesive ability, adsorbability and drug-carrying capability (LB de Paiva et al., 2008, RI ILIESCU et al., 2011, N Salahuddin et al., 2014). MMT is a FDA approved excipient having rich interlayer chemistry and high potential for ion exchange which use as pharmaceutical recipients, as active ingredients or as colloidal stabilizers in the emulsion. Clay minerals can be effectively modify drug release by delay (extended-release systems) drug release or even improve drug solubility (M Datta and M Kaur, 2014, C Aguzzi et al., 2007). The flexibility of interlayer spacing of layered silicates accommodates therapeutic agents, modify the suitability of some drugs for biological use and can later on be released to damaged cells (GV Joshi et al., 2009a, GV Joshi et al., 2009b). However, despite the beneficial effect of MMT, there are some inherent drawbacks associated

with the use of MMT for drug delivery. Under physiological conditions MMT dispersions tend to precipitate in ion containing solutions. The modification of the surface properties is of significance to widen the clay applications and has consequently received great concern (N Salahuddin et al., 2014, LB de Paiva et al., 2008). Although the modification of clay minerals can be achieved by various methods, the ion exchange of the inorganic cations with organic cations, usually with quaternary ammonium compounds, grafting clays with silanes and synthesis of polymer-clay nanocomposites would alleviate this disadvantage. In addition to exchangeable cations, the presence of OH groups at the broken edges of the clay sheets, furthermore presents a simple way to accommodate entities with particular functionalities on the clay exterior. Although Polymer-clay nanocomposites are frequently used as single drug carriers, this type of drug delivery system (DDS) (RI ILIESCU et al., 2011, GV Joshi et al., 2009a, A López-Galindo and C Viseras, 2004) often does not meet all requirements. Certain ailment situation and some chronic therapies need to use of two or multiple drugs to care for the diseases (K Karthikeyan et al., 2012). Investigation of novel methods and systems for ordered multiple-drug delivery in a sole formulation is a challenging, as well as important, aspect for smart drug delivery(R Salehi et al., 2015b). Cancer cells can increase resistance to chemotherapy drugs, but are less likely to develop resistance while multiple drugs are delivered concurrently, on the other hand, different drugs target different segments of the cancer cell (C-MJ Hu et al., 2010). Combination chemotherapy and nanoparticle drug delivery are two areas that have revealed major guarantee in cancer therapy. Combined treatment with two or more drugs elevates synergism between the different drugs against cancer cells and quenches drug resistance via different mechanisms of action. Nanoparticle drug delivery, conversely, improves therapeutic efficiency and diminishes toxic side effects. These two research fields have been lately combined to more progress the efficacy of cancer therapeutics (C-MJ Hu et al., 2010, T Okuda et al., 2010). On the other hand, the immune system of cancer patient in effect of chemotherapy become weak and they are susceptible to infectious diseases, so the during of chemotherapy for these patients, antibiotics be prescribed. The improvement of compounds with the capability to inhibit bacterial growth is a matter of major concern (M Rizzotto, 2012, H Zhu et al., 2013, VW Ng et al., 2014, AM Carmona-Ribeiro and LD de Melo Carrasco, 2013, J He et al., 2011). The research on the antimicrobial properties of montmorillonites modified with antibacterial agents, antibiotics, quaternary ammonium compounds and heavy metal ions (H Mahdavi et al., 2013, M

Parolo et al., 2011) has been center of attention because of the growing bacterial resistance due to the antibiotic overuse (M Parolo et al., 2011). Metallic ion-exchanged montmorillonite dispersed in water has revealed to absorbed bacteria by electrostatic forces (C-H Hu and M-S Xia, 2006). The aim of the present study was to develop a novel antibacterial nanocomposite to be used in combination cancer therapy. The physico-chemical characterization, in vitro release, antitumoral activity and microbiological efficacy of these nano-formulations were evaluated.

2. Experimental

2.1. Materials and methods

N-Isopropylacrylamide (NIPAAm) (99%, Sigma-Aldrich, Schnelldorf, Germany) was purified by recrystallization in n-hexane and then vacuum dried. Methyl iodide, N,N-dimethylaminoethyl methacrylate (DMAEMA) and Methacrylic acid (MAA) monomers (Sigma-Aldrich Co., Steinem, Germany) were purified by vacuum distillation. Ethylenediamine (EDA) (≥99%) was purchased from Merck Co. Cyanoguanidine , tetraethyl orthosilicate (TEOS), 3-amino propyltrimethoxysilane (3-ATMS),(3-chloropropyl) trimethoxysilane, absolute methanol, 1,4-dioxane, dimethylsolphoxide (DMSO) and n-hexane were purchased from Sigma-Aldrich (Steinem, Germany) and used as received. benzyl peroxide (BPO) (Sigma-Aldrich Co., Steinem, Germany) was employed as provided as an initiator. Doxorubicin hydrochloride and Methotrexate was obtained from Sobhan Pharmaceuticals, Iran and Zahravi Pharmaceuticals, Iran, respectively. MTT (3-(4, 5-dimethylthiazol-2-yl)-2, 5-diphenyltetrazolium bromide) and other biological reagents were obtained from Invitrogen (Carlsbad, CA). Other materials were of analytical grade and employed with no extra purification.

2.2. Synthesis

2.2.1. Synthesis of imidazolium-based ionic liquid (ImIL)

The synthesize procedure was described in previous work (S Rasouli et al., 2014b). (3-chloropropyl) trimethoxysilane (25.091 mmol) and 1-Methylimidazole (25.085 mmol) were mixed and refluxed at 80 ºC for three days under argon atmosphere. The orange suspension was filtered off and the solvent was evacuated. Then by addition of 100 mL dry dichloromethane, a precipitate became visible which was filtered off under argon atmosphere. The final product is then separated by distillation at 150 ºC under vacuum (1 mbar) and 1-methyl-3-(3-

trimethoxysilylpropyl) imidazolium chloride was achieved with a honey-like stability at room temperature (in 98% yield).

2.2.2. Synthesis of Imidazolium-modified mesoporous silica nanoparticles (ImIL-MSNs)

Hundred and seventy milliliter of ethanol and 7/2 mL TEOS were mixed in a 250 mL round bottom flask and 750µL (10 mmol) ammonia solution (37%) was added. Then, 60 mg 1-methyl-3-(3-trimethoxysilylpropyl) imidazolium chloride (ImIL) and 250 µl Ymethacryloxypropyltrimethoxysilane (MPS, 97 wt%) was added drop by drop and stirred for 72 h at room temperature. Then, product was cleansed with ethanol to eliminate excess of unreacted materials and vacuum dried (S Rasouli et al., 2014b).

2.2.3. Synthesis of cationic quaternary ammonium alkyl halide monomer (QDMAEMA)

Quaternary ammonium alkyl halide monomer (QDMAEMA) was prepared as described in previous work (R Salehi et al., 2015b). Firstly, 19.1 mmol of DMAEMA was added to 5 mL of dry THF during magnetic stirring, followed by dropwise addition of 22 mmol of CH_3I dissolved in 5 mL of THF. The reaction was performed for 12 h at ambient temperature with magnetic stirring. The products were filtered, washed with 15 mL cold hexane and vacuum dried for 8 h to obtain the DMAEMAQ product (white solid powder, yield: 95%).

2.2.4. Synthesis of organo-modified montmorillonite (OMMT)

Sodium montomorillonite clay (MMT) was pre-modified previous to being utilized in a dispersion polymerization procedure. The ImIL-MSNs modified montmorillonite (ImIL-MSNs-MMT) was prepared by adding a dispersed 1 g of sodium montmorillonite in 300 ml of deionized water at 50 °C into a solution of 1.1 g of ImIL-MSNs then ultrasonically dispersed for 5 min with sonication (400 W) by using probe-type ultrasonic generator. Then the resultant suspension was vigorously stirred for 72 hours. In this way the clay interlayers sodium ions exchanged by either cationic organic compound of imidazol or a cationic vinyl monomer, QDMAEMA. The precipitate was repeatedly filtered and washed with hot deionized water until all of chloride ion was removed (detected with 0.1 N $AgNO_3$ solutions). It was dried at 50 °C for 24 hours.

2.2.5. Synthesis of multifunctional stimuli-responsive nanocomposite with organo-modified montmorillonite

0.5 g of ImIL-MSNs-MMT added into 20 ml dioxane after 1 hour dispertion at 70- 80 ºC, N-isopropyl acryl amide (NIPAAm), metacrylic acide, N,N-dimethylaminoethyl methacrylate (QDMAEMA) with molar ratio of 50:40:10 and 2% w/w initiator (AIBN) was added initiator. The obtained mixture was placed in a clean polymerization tube, and the reaction mixture was degassed for 10 min with argon. Then, the tubes were sealed under argon atmosphere and the mixture polymerized for 48 h at 70–72 °C. After completion of reaction, the product P(NIPAAm-MAA-QDMAEMA)&ImIL-MSNs&MMT was rinsed and completely milled in a mortar to get fine powder.

2.3. Instrumentation

2.3.1. Fourier transforms infrared (FTIR) spectroscopy

The chemical structures of the synthesized P(NIPAAm-MAA-QDMAEMA)&ImIL-MSNs&MMT nanocomposites and DOX@MTX@CIP-loaded P(NIPAAm-MAA-QDMAEMA)&ImIL-MSNs&MMT nanocomposites were studied by FTIR spectroscopy (Equinox 55 LS 101, Bruker, Germany).

2.3.2. X-ray diffraction (XRD)

Powder X-ray diffraction patterns of the P(NIPAAm-MAA-QDMAEMA)&ImIL-MSNs&MMT nanocomposite were recorded on a Bruker AXS model D8 Advance diffractometer using CuKα radiation (λ=1.542A˚), with the Bragg angle ranging from 2–70°.

2.3.3. Scanning electron microscopy studies

The surface morphology, average diameter, particle size and pore volume of organo modified montmorilinite (OMMT) and P(NIPAAm-MAA-QDMAEMA)&ImIL-MSNs&MMT nanocomposites were assessed by a field emission scanning electron microscope-energy dispersive using X-ray (FESEM-EDX), S4160 Hitachi, Japan. Particle size was calculated by measuring the diameters of at least 50 particles revealed in SEM using image analysis software (Image-Pro plus 4.5; Media Cybernetics, Silver Spring, USA).

2.3.4. TGA

Thermogravimetric analysis (TGA) of P(NIPAAm-MAA-QDMAEMA)&ImIL-MSNs&MMT nanocomposites was carried out with a Mettler-Toledo model 822 instrument. Disintegration patterns of TGA were achieved under a nitrogen atmosphere at a heating rate of 10 °C per minute from 50 to 850 °C.

2.4. Preparation of inoculum

The standard strain of *P. aeruginosa* (ATCC: 25922*)* and *Escherichia coli* (ATCC: 27853) used in this project were obtained in lyophilized form from Institute of pasture, Iran. They were activated by culturing in sterile nutrient agar (liofilchem, Italy) for 48 hours at 37 °C. A single colony from grown plate was transferred into nutrient broth and incubated over night at 37 °C. Consequently after incubation time the cells were harvested by centrifugation at 1100 g for 10 min and rinsed two times and re-suspended in Ringer solution to provide an optical density of around 0.1 at 540 nm with a spectrophotometer (coleman, USA) or bacterial concentration around 10^8 CFU/ml.

2.5. Evaluation of the antimicrobial activity

The antimicrobial activities of prepared P(NIPAAm-MAA-QDMAEMA)&ImIL-MSNs&MMT and CIPRO@ P(NIPAAm-MAA-QDMAEMA)&ImIL-MSNs&MMT nanoformulations were studied by Minimum Inhibitory Concentration (MIC) determination against standard strain of *Pseudomonas aeruginosa* and *Escherichia coli* using the serial dilution method. Briefly bacterial inoculum in Muller-Hinton Broth medium in the concentrations equal to 0.5 of McFarland standard, added to serially diluted P(NIPAAm-MAA-QDMAEMA)&ImIL-MSNs&MMT NPs suspension with different concentrations of $195 – 1\times10^5$ $\mu g.mL^{-1}$ for *Escherichia coli* and *Pseudomonas aeruginosa,* CIPRO@ P(NIPAAm-MAA-QDMAEMA)&ImIL-MSNs&MMT with concentration in the range of 0.195 -12.5 $\mu g.mL^{-1}$ and 0.006 -3.125 $\mu g.mL^{-1}$ *fo*r *Pseudomonas aeruginosa* and *Escherichia coli,* respectively. After 24 h incubation at 37 ºC, from the content of the tubes streak cultures were made onto the Muller-Hinton agar plates. The first concentration with no bacterial growth on plates regarded as MIC. All tests were done in three separate occasions.

2.6. Drugs loading and release

300 mg P(NIPAAm-MAA-QDMAEMA)&ImIL-MSNs&MMT nanocomposite was ultrasonically dispersed in the 50 mg DOX solution for 5 min by using the probe-type ultrasonic generator(400 W). Then, it was stirred for 24 hours under dark conditions. DOX-loaded nanocomposite was collected by centrifugation at 23,000 g for 10 min in order to remove the unloaded DOX. After that, 10 mg MTX was added to DOX@MTX@ P(NIPAAm-MAA-QDMAEMA)&ImIL-MSNs&MMT mixture and dispersed with the help of ultrasonication (Sonics Vibra cell, Model: VCX 130 PB, Newton, CT) for 5 min(400 W). The mixture was stirred at room temperature for alternative 24 h under dark conditions. The unloaded MTX was removed by centrifugation at 23,000 g for 10 min. After that 10 mg CIPRO was added and the MTX&DOX-loaded nanocomposite mixture and stirred at room temperature for 24 h under dark conditions. CIPRO@MTX&DOX-loaded nanocomposite was collected by centrifugation at 23,000 g for 10 min and freeze dried. The obtained DOX&MTX-loaded nanocomposite was used for latter tests of in vitro drug release study and cytotoxicity test against T47D cell lines. The powdered CIPRO@MTX&DOX-loaded cationic dual thermo/pH-sensitive modified silica nanoparticles were dispersed in 3mL buffer solutions and poured into a dialysis membrane (MWCO 12,000 Da, Sigma–Aldrich, USA). The bag was afterward located in an 8mL of the same buffer solution of dialysis bag at 37 °C. The medium was placed into Incubator and stirred continuously during the release study. At suitable time periods, the whole solution (8 mL) was collected and meanwhile, 8 mL of the same fresh buffer solution was added and determined amounts of released DOX, MTX and CIPRO in the original buffer solutions. It should be noted that three different pH values of 4, 5.8 and 7.4 were utilized to imitate the different biological situations. The relative percentage of the released DOX and MTX were computed as a function of incubation time based on the amount of the existing drug in the nanoparticles. The HPLC-UV method was used for measurement amounts of DOX, MTX and CIPRO released at wavelength of 227, 300 and 267 nm as previously described (R Salehi et al., 2015b, S Davaran et al., 2015). In order to reduce error, all measurements were repeated twice. Percentage of drug released from the nanocomposite was obtained using the following formula:

$$\text{Drug encapsulation efficiency (\%, w/w)} = \frac{Mass\ of\ drug\ in\ nanogels}{Mass\ of\ feed\ drug} \times 100$$

$$\text{Drug loading efficiency (\%, w/w)} = \frac{Mass\ of\ drug\ in\ nanogels}{Mass\ of\ nanogels} \times 100$$

$$\text{Drug released\%} = \frac{\text{amount of drug in release medium}}{\text{amount of drug in nano formulation}} * 100$$

2.7. Cell culture and In vitro cytotoxicity assay

T47D cell line were obtained from National Cell Bank of Iran and maintained in 75 cm^2 culture flask, in Roswell Park Memorial Institute 1640 medium (RPMI 1640 medium; Gibco BRL Life Technologies) supplemented with 10% (v/v) fetal bovine serum and antibiotics (100 mg/ml penicillin–streptomycin). The cells were incubated at 37 °C in an atmosphere of 5% CO_2 and 95% air with more than 95% humidity; medium was changed every two days for cell feeding. T47D cell lines were used as the target cells and were used to evaluate the cytotoxicity of nano carriers using MTT assay. Also the antitumor activity of the DOX@MTX-loaded P(NIPAAm-MAA-QDMAEMA)&ImIL-MSNs&MMT was assessed by MTT method as previously described (S Rasouli et al., 2014a). Briefly, when cell population reached to 70 % confluence, they were dissociated with 0.25% trypsin in PBS (pH 7.4) and centrifuged at 800 g for 7 min at room temperature. Then inoculated in 96-well microplates with a cell density of 5×10^3 cells per well in 180 µL RPMI 1640, and incubated in a humidified atmosphere containing 5% CO_2 at 37 °C for 24 h to allow the cells to attach to the bottom of the well. In this context, different concentration (20, 10, 5 and 2.5 µg/mL) of drug-loaded nanocarriers and pure drug were prepared in fresh cell growth medium and administered into the wells with different time's manners. Drug-free nanocarriers with concentration of 1000 µg/mL were seeded to investigate the cytotoxicity of nanocarrier. After incubation for a predetermined time, a microplate was withdrawn for MTT assay. The MTT assay was done as follows: 20 µL of MTT solution (5mg /2ml) in PBS (pH 7.4) was added to all wells. The incubation was done for a further 4 h and then the solution was removed carefully from wells and then the cells treated with Sorenson buffer. After treating, the optical density of every well was read using a microplate reader (Multiskan MK3, Thermo Electron Corporation, USA) at a wavelength of 570 nm, and growth inhibition was calculated. All of the tests were repeated for three times and statistical analyses were performed using SPSS 15; $p < 0.05$ was considered significant.

2.8. QRT-PCR

The T47D cells seeded in 6-well plates were treated with different doses (10, 100, and 250 µg/ml) of both DOX@MTX-loaded P(NIPAAm-MAA-QDMAEMA)&ImIL-MSNs&MMT (PD) and free combination of DOX@MTX (D) for 48 hours in 37ºC, 5% CO_2, and enough humidified incubator. Non-treated cells used as control. The total cellular RNA was extracted from each treatment using MiRCURY RNA isolation Kit cell and plant (Exiqon, Denmark) according to the manufacturer's recommendations. Reverse transcription of isolated RNAs were performed using Revert Aid cDNA synthesis kit (Fermentas, USA). Real-time PCR reactions were runned using a Master SYBR Green (Jena Bioscience, Germany) on a Rotor gene 6000 (Corbett, Australia) real time instrument. The data were normalized to an endogenous control gene (GAPDH) and calibrated to non-treated (control) cells. All reactions were performed in triplicate. For data analysis comparative threshold cycle method was used. The specific primers were summarized in Table 1.

Table 1

2.9. Statistical analysis

Analysis of variance (ANOVA) and Student's t test were used to determine the significant differences among groups. The difference was considered statistically significant at p values less than 0.05. Our data were shown as mean± standard deviation (SD).

3. Results and discussion

The synthesized root of novel multifunctional P(NIPAAm-MAA-QDMAEMA)&ImIL-MSNs&MMT carrier are shown schematically in Figure 1.

Figure 1

3.1. Characterization

3.1.1. Fourier transforms infrared spectroscopy

The chemical structures of the P(NIPAAm-MAA-QDMAEMA)&ImIL-MSNs&MMT (Figure 2a) and DOX@MTX@CIP@ P(NIPAAm-MAA-QDMAEMA)&ImIL-MSNs&MMT (Figure 2b) were studied by FTIR spectroscopy. The existence of MMT (Figure 3a) was characterized by the stretching and bending vibrations of Si-O-Si and Si-O-Al, at 1044 cm^{-1} and 524 cm^{-1}, respectively. Stretching vibration of Al-Al-OH moieties in the octahedral layer was observed at 816 cm^{-1}. Interlayer water was apparent by the broad –O-H peak at 3452 cm^{-1}. The band at 3698 cm^{-1} was attributed to the stretching band of –OH at Al-OH and that of Si-OH as well as

Interlayer water. The –OH bending mode of absorbed water was indicated as a series of over lied bands at 1638 cm^{-1}. The broad absorption bands at 1725 cm^{-1} could be attributed to the stretching vibration of carbonyl groups in MAA and DMAEMAQ moiety of copolymer. Absorption bands at 1641 cm^{-1} must be due to the stretching vibration of C=O of amide at NIPAAM moiety of copolymer as well as aromatic C=C of MPS and imidazolium ring. The peak at 1522 cm^{-1} was also attributed to stretching vibration of C=N of imidazolium aromatic ring. The C–H stretching vibration of the aliphatic and aromatic ring was manifested through strong peak at 2950-3087 cm^{-1}.

The FTIR spectra of DOX@MTX@CIP-loaded P(NIPAAm-MAA-QDMAEMA)&ImIL-MSNs&MMT (Figure 2b) revealed a new peak at 1750 cm^{-1} that was related to carbonyl groups of cyclohexanone ring of doxorubicin. Peaks at 1665 and 1535 cm^{-1} was assigned to stretching vibration of quinolones in CIP and amines bending vibration of MTX. The peak at 1720 cm^{-1} was weakened because of ionic interaction between the drug and carrier. Therefore, the FTIR results proved the successful encapsulation of drugs on the carrier.

Figure 2

3.1.3. XRD

Montmorilonite was modified with multifunctional P(NIPAAm-MAA-QDMAEMA)&ImIL-MSNs&MMT nanocomposite. XRD pattern was used to demonstrate this modification. At $2\theta = 7.69°$ the basic spacing of Montmorilonite (MMT) was 11.48 nm but following the modification this angle moved to $2\theta = 5.78°$ and basic spacing of planes altered to 15.27 nm (Figure 3). According to the Bragg's law, the peak altering from upper refraction angle to lower refraction angle is due to increase in the d-spacing which indicates that P(NIPAAm-MAA-QDMAEMA)&ImIL-MSNs has been effectively intercalated into the interlayer of MMT (Figure 1) and is lying flat on the surface of MMT as monolayer (G Lagaly and I Dékany, 2005, KS Katti et al., 2010).

Figure 3

3.1.4. Morphology

Figure 4 and 5 presents the SEM micrographs of organo modified montmorilinite (OMMT) (Figure 4a) and P(NIPAAm-MAA-QDMAEMA)&ImIL-MSNs&MMT (Figure 5a). The particles sizes were in the range of 30-100 nm. EDX spectrums of OMMT (Figure 4b) and P(NIPAAm-MAA-QDMAEMA)&ImIL-MSNs&MMT (Figure 5b) confirmed the presence of all

elements that were predicted to attend at the structure of OMMT and final nanocomposite. In Figure 4b the intensity of Al peaks at OMMT was much more than other elements but at final nanocomposite due to the addition of polymeric comportment to nanocomposite, the intensity of Al peaks was decreased but the intensity of Si, C, N and O increased (Figure 5b).

Figure 4

Figure 5

3.1.4. Thermal analysis

Figure 6 depicted the thermogravimetric analysis (TGA) profile for P(NIPAAm-MAA-QDMAEMA)&ImIL-MSNs&MMT nanocomposite. TGA thermograms of nanocomposite showed weight loss in four steps in the temperature region of 80–150, 200–300, 300-450 and 600–750 ºC. It is explicable that decomposition of intercalated organic parts (imidazolium part and polymeric blocks) took place in the temperature range of 200–450 ºC resulting in two strong endothermic peaks at this temperature range. This stage of weight loss between is attributed to the combustion (The maximum weight loss) of organic part (60 % weight loss). The maximum rate degradation temperature (Tmax, first derivative peak temperature) was 250 ºC. A weight loss at 80-150 and 650 ºC is due to evaporation of adsorbed water and organic solvents and loss of structural hydroxyl group (HC Bajaj and RV Jasra, 2007).

Figure 6

3.2. Drug loading

It was reported that drug incorporation into clays takes place by adsorption, both by intercalation into the clay composition within the interlayer spacing (by substitution with the water molecules), and moreover on the exterior. The most significant exchanges proceeding among the two sections of the system are ionic (RI ILIESCU et al., 2011). The ionic replacement process may occur by mixing ion exchangers with ionic drugs in solution. The positively charged boundaries on the layers of MMT can interact with anionic fractions of all of three drugs. MMT also contains dangling hydroxyl end-groups on the surfaces (H Khalil et al., 2005). In this study smart multifunctional nanocarrier P(NIPAAm-MAA-QDMAEMA)&ImIL-MSNs&MMT of different functional groups with potent ability to simultaneous interaction by multiple drugs DOX, MTX and CIP were developed. DOX is a weak base is able to interact strongly with ion-exchange mechanism and hydrogen bonds to modified NPs synthesized here. MTX also is able to ionic interaction with positively charged component of carrier and the formation of strong

hydrogen bonds. The drugs loading experiments were performed at pH 7.4. At pH of 7.4, free surface silanol groups of MSNs with pKa= 6.8 (S Rasouli et al., 2014b) are negative charged also carboxylic acid groups of grafted PMAA in the carrier are deprotonated (pKa=6) (R Salehi et al., 2015a) and thereupon negatively charged. On the other hand, QDMAEMA part of NPs and edges on the layers of MMT has positively charged(R Salehi et al., 2015b, J Chen et al., 1990). DOX with pKa=8.3 at pH=7.4 is positively charged (R Salehi et al., 2014, R Salehi et al., 2015a). MTX was another drug that was used in our study. At pH of 7.4, the net charge of MTX was negative because pKa of MTX is 3.8, 4.8 and 5.6 (S Rasouli et al., 2014b).CIP an antibacterial agent was selected as the third drug in this study. The pKa value of the antimicrobial drug, CIP is 6.09 for carboxylic acid group and 8.74 for the nitrogen on the piperazinyl ring (S Davaran et al., 2015). At pH 7.4, the acid will be primarily dissociated and the nitrogen will be primarily protonated. Therefore, CIP had both negative and positive charge. The DOX, MTX and CIP were loaded by the composite nanoparticles (Figure 7) by following reasons: a) electrostatic attraction between anionic and cationic parts of nanocomposite and drugs, b) hydrogen bonding, c) intercalation into the clay structure, d) ionic exchange between clay cations and cationic part of drugs and e) existence of electrostatic interactions among the protonated amino parts of the DOX and CIP cations and the anionic charges at surface of the MMT. Therefore, the synthesized carrier could be increased encapsulation efficiency. The drug loading results indicated that conjugation of DOX in modified NPs did not affect the loading capacity of nanoparticles for conjugation with second and third drugs MTX and CIP. As well as all of drugs were loaded separately with more than around 95% encapsulation efficiency. In addition, our developed delivery system needed low amount of carrier for efficient drug delivery because of high loading efficiency values. In this report the simultaneous loading of multiple anticancer drugs, DOX, MTX and CIP was obtained to explore potential combination therapy applications.

Figure 7

3.3. In vitro drug release study

To achieve successful anticancer drug delivery, a drug needs to be avoided from release in physiological condition (normal tissues) and then be released into the tumor tissue, which is considered the optimum site for targeted delivery of anticancer drugs. The sustained release of drugs from the nanoparticles is an essential requirement for cancer therapy (A Singh et al.,

2011). As previously mentioned, most cancer tissues have lower extracellular pH values than normal tissues. Therefore pH-sensitive NPs are in the center of interests in cancer research. Figure 8 showed the drug release curves of multi drug loaded smart P(NIPAAm-MAA-QDMAEMA)&ImIL-MSNs&MMT nanocomposite, incubated in a simulative normal body fluid (50 mM PBS, pH 7.4) and an acidic environment (50 mM PBS, pH 5.8 and 4) for 25 days at 37 °C. The release profile for P(NIPAAm-MAA-QDMAEMA)&ImIL-MSNs&MMT NPs was studied at three stages: initial burst release at first 24 h (stage I), then fast release from 24-300 h (stage II), followed by a decelerating release and finally constant release from 300-600 h (stage III). The release was found to follow a diffusing way at the initial stages of the release (first 24 h), that around 5-15% of DOX and MTX were released no matter in buffer with natural or mild acidic pH. In the initial stage (first 24h) at 37 ºC and pH 5.8 and 7.4, a negligible CIP was released (around 4%) from P(NIPAAm-MAA-QDMAEMA)&ImIL-MSNs&MMT NPs. There was a high concentration gradient between the hydrogel surface and the release medium. Considering that it is the driving force for drug diffusion at first 24h. Also the part of drugs that physically loaded on NPs released in this stage. After the burst period, a significant pH-dependent release response can be observed for all of three drugs at stage II. In this stage the part of DOX, MTX and CIP started to release that loaded by pH-dependent ionic interaction and hydrogen bonding in NPs. The multiple drugs released separately and released amount reached 70–85% at pH values of 5.8 and 4 (stage II), except CIP release at pH 5.8 that remained constant and did not increased more than 20% up to end of the release study. After 300 h, small amount of drugs released from the NPs (only 5-10%). There was a slight difference in the release profile and rate of the two anticancer drugs, MTX and DOX, at pH values of 4 and 5.8. At the end of the release study the percentage of DOX, MTX and CIP was only 10-20% at pH 7.4. Furthermore, CIP released at both mentioned pHs (5.8 and 7.4) was negligible. By decreasing the pH value, an obvious increase in the drug release rate can be observed. The mutual interactions between the drugs and the P(NIPAAm-MAA-QDMAEMA)&ImIL-MSNs&MMT NPs influence the differences in the release profiles for the drugs. In fact, interactions between amine, hydroxyl and carboxylic groups in the drugs and in the NPs have been proven to entrap and greatly restrict the remaining drug from releasing. Carrier/drugs interactions decrease the drug release rate by increasing drug/carrier adsorption capacity/entrapment efficiency (T Pongjanyakul and H Suksri, 2009). The multiple-drug release behavior is ascribed to their special structures. DOX, MTX and

CIP shows the degree of ionization depends on pH conditions. There is repulsive force among drugs and NPs, at mild acidic condition cause the multilayer covering loose and drugs releases from the DDDS. However, at pH 7.4, electrostatic interaction between MTX, DOX and the multifunctional NPs (for CIP at both pHs 5.8 and 7.4) let to negligible drug release from P(NIPAAm-MAA-QDMAEMA)&ImIL-MSNs&MMT NPs. This could be a possible reason for depot or reservoir effect of our newly prepared formulation to simultaneous release the multiple drugs in longer time intervals.

This property of P(NIPAAm-MAA-QDMAEMA)&ImIL-MSNs&MMT NPs should be very useful to effectively treat tumors with acidic microenvironments and reduce the side effects of the drug on the normal tissues.

Figure 8

3.4. In-vitro antibacterial efficiencies of Novel developed nanoparticles The multifunctional P(NIPAAm-MAA-QDMAEMA)&ImIL-MSNs&MMT nanocomposites synthesized here have cationic quaternary amine block intercalated in MMT that is known to have antibacterial property (M Parolo et al., 2011, G Vigliotta et al., 2012, M Mohammed et al., 2010, J He et al., 2011). Therefore we expected that the novel developed nanoparticles here had potent antibacterial ability. To test this hypothesis, we performed the antibacterial test of novel developed nanoparticles against standard strains of *Pseudomonas aeruginosa* and *Escherichia coli*. The mentioned bacteria's treated with P(NIPAAm-MAA-QDMAEMA)&ImIL-MSNs&MMT and of CIP@ P(NIPAAm-MAA-QDMAEMA)&ImIL-MSNs&MMT nanocomposites of various concentrations (Table 2) to study the antibacterial activity. The results indicated that the novel developed nanoparticle had antibacterial ability. A blank sheet without polymer vesicles was used as the control to compare the antibacterial activity. The antibacterial photographs were taken after incubation for 48 h at 37 ºC. Figure 9 depicts the results of streak cultures on the surfaces of Muller-Hinton agar plates, the first concentration with no mark of bacterial growth on plates considered as MIC. As shown in Figure 9, dense bacterial colonies were monitored in the control sample with no vesicle treatment, Moreover, no bacterial growth was observed for *Escherichia coli* (Figure 9b) treated with 195 $\mu g.mL^{-1}$ confirming the enhanced antibacterial activities of novel developed nanoparticle sample, P(NIPAAm-MAA-QDMAEMA)&ImIL-MSNs&MMT, against *Escherichia coli*. But the and

P(NIPAAm-MAA-QDMAEMA)&ImIL-MSNs&MMT nanocomposite did not show any antibacterial ability when treated with *Pseudomonas aeruginosa* at concentration range of 195 – 1×10^5 µg.mL^{-1} (Figure 9a). MIC values of CIP@P(NIPAAm-MAA-QDMAEMA)&ImIL-MSNs&MMT nanocomposite were measured to be 1.56 and 0.048 µg.mL^{-1} for *Pseudomonas aeruginosa*(Figure 9c) and *Escherichia coli* (Figure 9d), respectively. The resultant products are effective in controlling the growth of bacteria. It is also found that the MIC of novel developed nanoparticle as antimicrobial agent varies based on the microorganism species.

Table 2

Figure 9

3.5. In vitro cell assay

In order to study the anti-proliferation efficacy of the novel developed dual anticancer drug loaded nanocomposite, free DOX@MTX and DOX@MTX@ P(NIPAAm-MAA-QDMAEMA)&ImIL-MSNs&MMT with concentrations range from 5 to 100 µg/mL were exposed to T47D breast cancer cells for 72 h, and the cell viabilities were quantified by MTT assay (Figure 10). This dual anticancer drugs, DOX@MTX cytotoxicity in free form or loaded in NPs was increased in dose-dependent manner which lower cancer cell viability was achieved by decreasing drug concentration. The blank carrier of P(NIPAAm-MAA-QDMAEMA)&ImIL-MSNs&MMT nanocomposites revealed biocompatibility and had a high viability (above 78 and 90%) cells at 250-1000 µg/mL after 72 h exposure on the T47D cells. Significant growth inhibition of T47D cells was observed when the cells were treated with either the suspension of DOX@MTX-loaded P(NIPAAm-MAA-QDMAEMA)&ImIL-MSNs&MMT nanocomposites or pure DOX and MTX . Only 21 and 12 % of the cells remained viable at a DOX@MTX dose of 5 µg.mL after incubation with free DOX@MTX and DOX@MTX-loaded nanocomposite, respectively. Hence, DOX@MTX antitumor efficacy was maintained while encapsulated in nanoparticles. The cell viability of dual drug-loaded NPs was much higher than that of free drugs. This might be due to the sustained release of DOX@MTX from DOX@MTX-loaded nanocomposite, inducing a higher cell death.

Figure 10

3.6. Quantitative real-time PCR (qPCR):

The cyclin D1 is a biomarker of turmeric phenotype and progression(EA Musgrove et al., 2011). Therefore, is considered a therapeutic target for cancer. Cyclin D1 plays an important role in G1 phase of cell cycle progression. Forced expression of cyclin D1 results in reduction in cell size, shortens the G1 phase in cell cycle, and leads to the oncogenic transformation of the cells (JP Alao, 2007). In addition to regulation of cell proliferation, Cyclin D1 controls senescence, tumourigenesis, and apoptosis. The cyclin D1 over-expression can lead to apoptosis resistance in cell lines(G Roue et al., 2008). In this study, we investigated the expressions of cyclin D1 after each treatment in T47D cell line to know if our nanocomposite can reduce cyclin D1 expression in accordance with its anti-proliferative and cytotoxic activities. Quantitative transcriptional evaluation of cyclin D1 in both D and PD treated cells revealed down regulation of cyclin D1 gene in comparable levels, but the statistical analysis showed that the reduction is much higher in PD treated cells ($p<0.01$) (Figure 11). This means that our PD has an effective anti-cancer as well as anti-proliferative activity

Figure 11

Conclusion

Combination chemotherapy and nanoparticle drug delivery are two areas that have revealed considerable promise in cancer treatment. Combined therapy of two or more drugs increases synergism among the different drugs against cancer cells. Nanoparticle drug delivery, on the other hand, enhances therapeutic effectiveness, reduces side effects of the drug payloads by unprecedented level of control over the pharmacokinetics of chemotherapeutic agents. Polymer-clay nanocomposites are highly sought-after materials, mainly due to their applicability in a variety of avenues. In addition, emerging techniques in drug–polymer conjugations and nanomaterials engineering will continue to expand the nanoparticle platforms on which better therapeutic regimens can be designed. A novel multiple drug loaded polymeric-modified clay composed of P(NIPAAm-MAA-QDMAEMA)&ImIL-MSNs&MMT nanocomposites was developed and assessed for efficacy and suitability in guided drug delivery systems. XRD patterns of hybrid material shows an increase in the d-spacing, conforming the intercalation of copolymeric part into the interlayer of MMT. TGDTA of nanocomposite shows a sharp weight loss at about 250-450 ºC due to decomposition of exchanged copolymer. This polymeric-modified clay showed suitable inhibition properties over *Escherichia coli* growth and can be considered to be an interesting material for scientific research of antibacterial composites. This

formulated drug carrier system provided the opportunity to deliver multiple drugs in combination in a sustained, pH dependent release manner, substantiating dose-dependent cytotoxic activity in T47D cells. Persistent growth of such combination delivery systems will eventually lead toward accessibility of efficient therapies for cancer.

References

Aguzzi C, Cerezo P, Viseras C & Caramella C, *Applied Clay Science*, 2007. **1**, 36:22;

Alao J P, *Molecular cancer*, 2007. 6:24;

Bajaj H C & Jasra R V, *Current Science*, 2007. **7**, 92:1005;

Carmona-Ribeiro A M & De Melo Carrasco L D, *International journal of molecular sciences*, 2013. **5**, 14:9906;

Chen J, Cushman J H & Low P, *Clays and Clay Minerals*, 1990. **1**, 38:57;

Darehkordi A, Hosseini S & Tahmooresi M, *Iranian Journal of Materials Science & Engineering*, 2012. **3**, 9;

Datta M & Kaur M, *Int J Pharm Pharm Sci*, 2014. **5**, 6:100;

Davaran S, Lotfipour F, Sedghipour N, Sedghipour M R, Alimohammadi S & Salehi R, *Journal of microencapsulation*, 2015. **5**, 32:511;

De Paiva L B, Morales A R & Díaz F R V, *Applied Clay Science*, 2008. **1**, 42:8;

He J, Söderling E, Österblad M, Vallittu P K & Lassila L V, *Molecules*, 2011. **11**, 16:9755;

Hu C-H & Xia M-S, *Applied Clay Science*, 2006. **3**, 31:180;

Hu C-M J, Aryal S & Zhang L, *Therapeutic delivery*, 2010. **2**, 1:323;

Iliescu R I, Andronescu E, Daniela C, Ghiţulică D B & Ficai A, *UPB Scientific Bulletin, Series B*, 2011. **3**, 73;

Joshi G V, Kevadiya B D, Patel H A, Bajaj H C & Jasra R V, *International Journal of Pharmaceutics*, 2009a. **1**, 374:53;

Joshi G V, Patel H A, Kevadiya B D & Bajaj H C, *Applied Clay Science*, 2009b. **4**, 45:248;

Karthikeyan K, Guhathakarta S, Rajaram R & Korrapati P S, *International Journal of Pharmaceutics*, 2012. **1**, 438:117;

Katti K S, Ambre A H, Peterka N & Katti D R, *Philosophical Transactions of the Royal Society of London A: Mathematical, Physical and Engineering Sciences*, 2010. **1917**, 368:1963;

Khalil H, Mahajan D & Rafailovich M, *Polymer international*, 2005. **2**, 54:423;

Lagaly G & Dékany I, *Advances in colloid and interface science*, 2005. 114:189;

López-Galindo A & Viseras C, *Interface Science and Technology*, 2004. 1:267;

Mahdavi H, Mirzadeh H, Zohuriaan-Mehr M J & Talebnezhad F, *J Am Sci*, 2013. 9:203;

Mohammed M, Tahar B, Aïcha D & Eddine H D, *Journal of Chemistry*, 2010. **S1**, 7:S61;

Musgrove E A, Caldon C E, Barraclough J, Stone A & Sutherland R L, *Nat Rev Cancer*, 2011. **8**, 11:558;

Negrete-Herrera N, Putaux J-L & Bourgeat-Lami E, *Progress in Solid State Chemistry*, 2006. **2**, 34:121;

Ng V W, Chan J M, Sardon H, Ono R J, García J M, Yang Y Y & Hedrick J L, *Advanced drug delivery reviews*, 2014. 78:46;

Okuda T, Tominaga K & Kidoaki S, *Journal of Controlled Release*, 2010. **2**, 143:258;

Parolo M, Fernández L, Zajonkovsky I, Sánchez M & Bastion M, *Science against microbial pathogens: communicating current research and technological advances. Formatex, Microbiology series*, 2011. 3:144;

Pongjanyakul T & Suksri H, *Colloids and Surfaces B: Biointerfaces*, 2009. **1**, 74:103;

Rasouli S, Davaran S, Rasouli F, Mahkam M & Salehi R, *Designed Monomers and Polymers*, 2014a. **3**, 17:227;

Rasouli S, Davaran S, Rasouli F, Mahkam M & Salehi R, *Drug delivery*, 2014b. **3**, 21:155;

Rizzotto M 2012. *Metal complexes as antimicrobial agents*, INTECH Open Access Publisher.
Roue G, Pichereau V, Lincet H, Colomer D & Sola B, *Oncogene*, 2008. **36**, 27:4909;

Salahuddin N, Elbarbary A, Allam N G & Hashim A F, *Journal of Applied Polymer Science*, 2014. **23**, 131;

Salehi R, Irani M, Eskandani M, Nowruzi K, Davaran S & Haririan I, *International Journal of Polymeric Materials and Polymeric Biomaterials*, 2014. **12**, 63:609;

Salehi R, Rasouli S & Hamishehkar H, *Int. J. Pharm*, 2015a. **1**, 487:274;

Salehi R, Rasouli S & Hamishehkar H, *International Journal of Pharmaceutics*, 2015b. **1**, 487:274;

Singh A, Dilnawaz F, Mewar S, Sharma U, Jagannathan N & Sahoo S K, *ACS APPL MATER INTER* 2011. **3**, 3:842;

Thomas P C, Cipriano B H & Raghavan S R, *Soft Matter*, 2011. **18**, 7:8192;

Vigliotta G, Mella M, Rega D & Izzo L, *Biomacromolecules*, 2012. **3**, 13:833;

Zhu H, Geng Q, Chen W, Zhu Y, Chen J & Du J, *J. Mater. Chem. B*, 2013. **40**, 1:5496;

Table Caption

Table 1. Primer sequences for qRT-PCR

Table 2. Results of Minimum Inhibitory Concentration (MIC) determination ($\mu g.mL^{-1}$) of P(NIPAAm-MAA-QDMAEMA)&ImIL-MSNs&MMT and Ciprofloxacin loaded P(NIPAAm-MAA-QDMAEMA)&ImIL-MSNs&MMT Nanocomposite

Figure Caption

Figure 1. Synthesis root of P(NIPAAm-MAA-QDMAEMA)&ImIL-MSNs&MMT

Figure 2. FTIR spectra of a) P(NIPAAm-MAA-QDMAEMA)&ImIL-MSNs&MMT, and b) DOX@MTX@CIP loaded P(NIPAAm-MAA-QDMAEMA)&ImIL-MSNs&MMT

Figure 3. XRD pattern of P(NIPAAm-MAA-QDMAEMA)&ImIL-MSNs&MMT

Figure 4. SEM (a) and EDX (b) images of organo modified montmorilinite (OMMT)

Figure 5. SEM (a) and EDX (b) images of P(NIPAAm-MAA-QDMAEMA)&ImIL-MSNs&MMT

Figure 6. TGA thermogram of P(NIPAAm-MAA-QDMAEMA)&ImIL-MSNs&MMT nanoparticles

Figure 7. Scheme of simultaneous loading of multiple anticancer drugs including doxorubicin (DOX) and methotroxate (MTX) on pH-responsive P P(NIPAAm-MAA-QDMAEMA)&ImIL-MSNs&MMT nanoparticles

Figure 8. Cumulative release of doxorubicin (DOX), methotroxate (MTX) and ciprofloxacine (CIP) from DOX@MTX@CIP loaded pH-responsive P(NIPAAm-MAA-QDMAEMA)&ImIL-MSNs&MMT nanoparticles at different pH (4 , 5.5 and 7.4) 37 °C

Figure 9.Streak cultures on the surfaces of Muller-Hinton agar plates, P(NIPAAm-MAA-QDMAEMA)&ImIL-MSNs&MMT treated with a)*Pseudomonas aeruginosa*, b) *Escherichia coli* and CIP@ P(NIPAAm-MAA-QDMAEMA)&ImIL-MSNs&MMT treated with

c)*Pseudomonas aeruginosa*, d) *Escherichia coli* .The first concentration with no sign of bacterial growth on plates considered as Minimum Inhibitory Concentration (MIC)

Figure 10. Cell growth inhibition rates by different concentration of MTX@DOX@Carrier and MTX@DOX on T47D cell lines after 72 h incubation

Figure 11. Relative transcriptional evaluation of cyclin D1 in T47D cells after treatments with D: free MTX/DOX and PD:(DOX@MTX-loaded P(NIPAAm-MAA-QDMAEMA)&ImIL-MSNs&MMT) transcriptional reduction in cyclin D1 was observed in both PD and D treated cells but down regulation is significantly higher in PD treatments. Asterisk shows significant difference between the groups for cyclin D1 **: P<0.01.

Table 2. Primer sequences for qRT-PCR

Cyclin D1	Forward: TGCCCTCTGTGCCACAGATG
	Reverse: TCTGGAGAGGAAGCGTGTGA
GAPDH	Forward: GGGTGTGAACCATGAGAAGT
	Reverse: GGCATGGACTGTGGTCATCA

Table 2. Results of Minimum Inhibitory Concentration (MIC) determination ($\mu g.mL^{-1}$) of P(NIPAAm-MAA-QDMAEMA)&ImIL-MSNs&MMT and Ciprofloxacin loaded P(NIPAAm-MAA-QDMAEMA)&ImIL-MSNs&MMT Nanocomposite

	Escherichia coli		*Pseudomonas aeruginosa*	
	Concentrations ($\mu g.mL^{-1}$)	MIC*	Concentrations ($\mu g.mL^{-1}$)	MIC*
P(NIPAAm-MAA-QDMAEMA)&ImIL-MSNs&MMT Nanocomposite	195 – 1×10^5 $\mu g.mL^{-1}$	195 $\mu g.mL^{-1}$	195 – 1×10^5 $\mu g.mL^{-1}$	-
Ciprofloxacin loaded P(NIPAAm-MAA-QDMAEMA)&ImIL-MSNs&MMT Nanocomposite	0.006 - 3.125 $\mu g.mL^{-1}$	0.048 $\mu g.mL^{-1}$	0.195-12.5 $\mu g.mL^{-1}$	1.56 $\mu g.mL^{-1}$

* All MIC experiences were repeated for three times and mean of the results were considered as the final MIC.

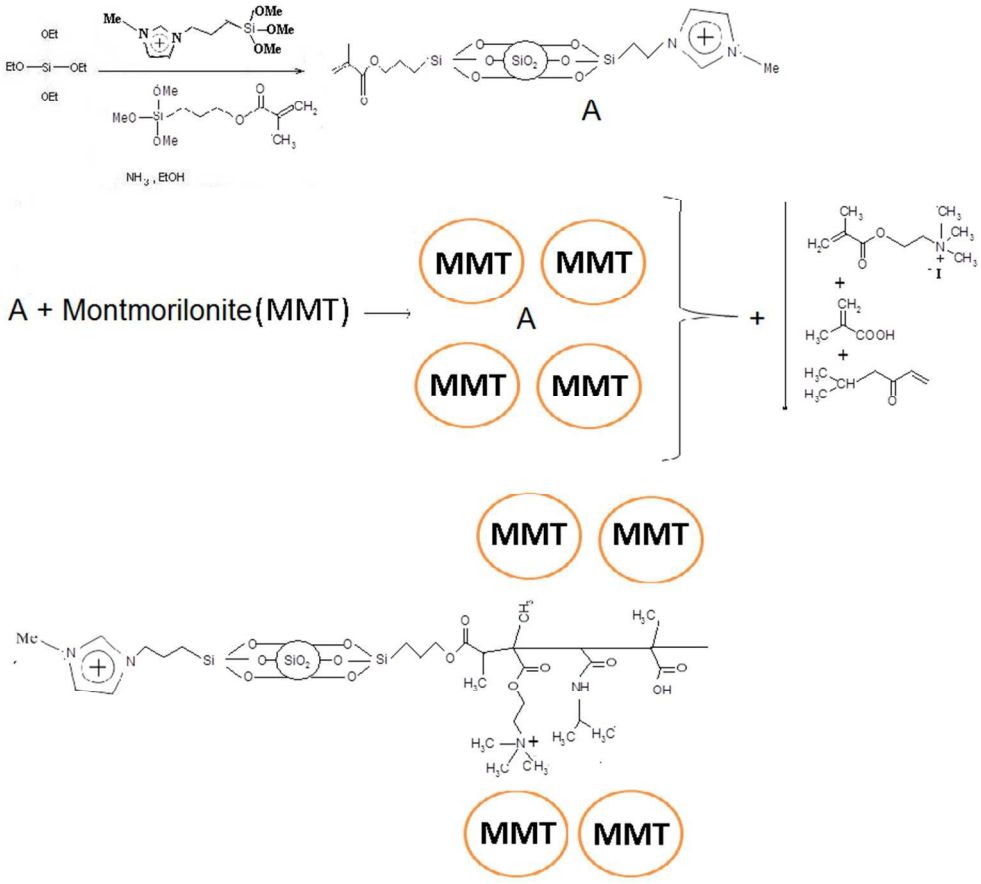

247x218mm (96 x 96 DPI)

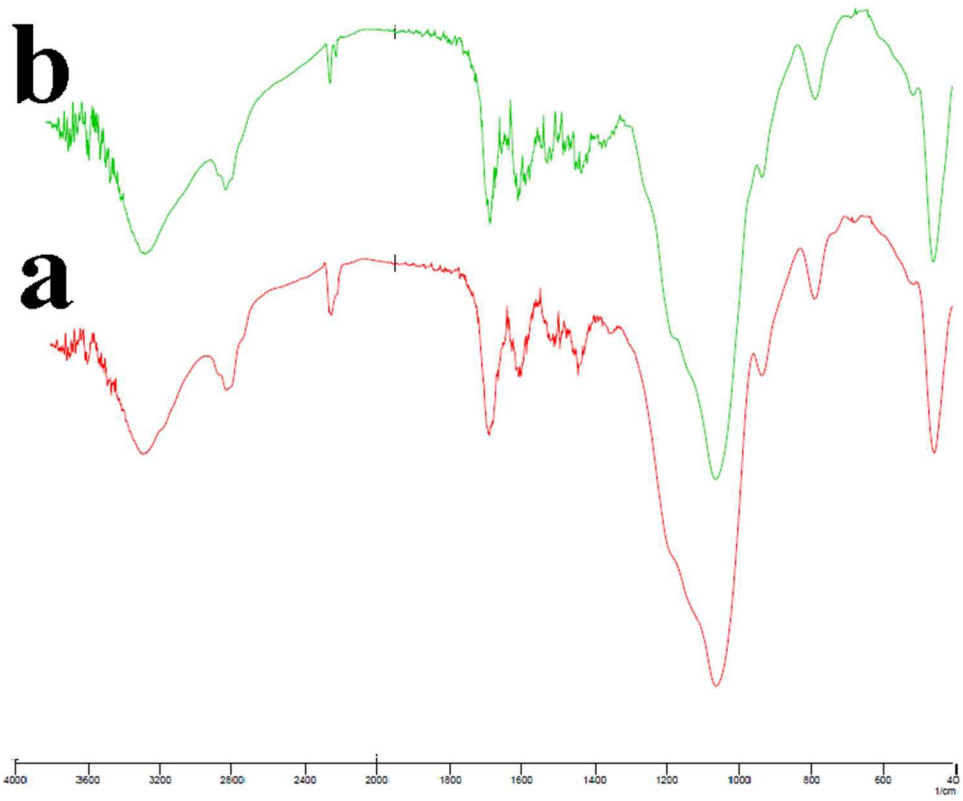

216x183mm (96 x 96 DPI)

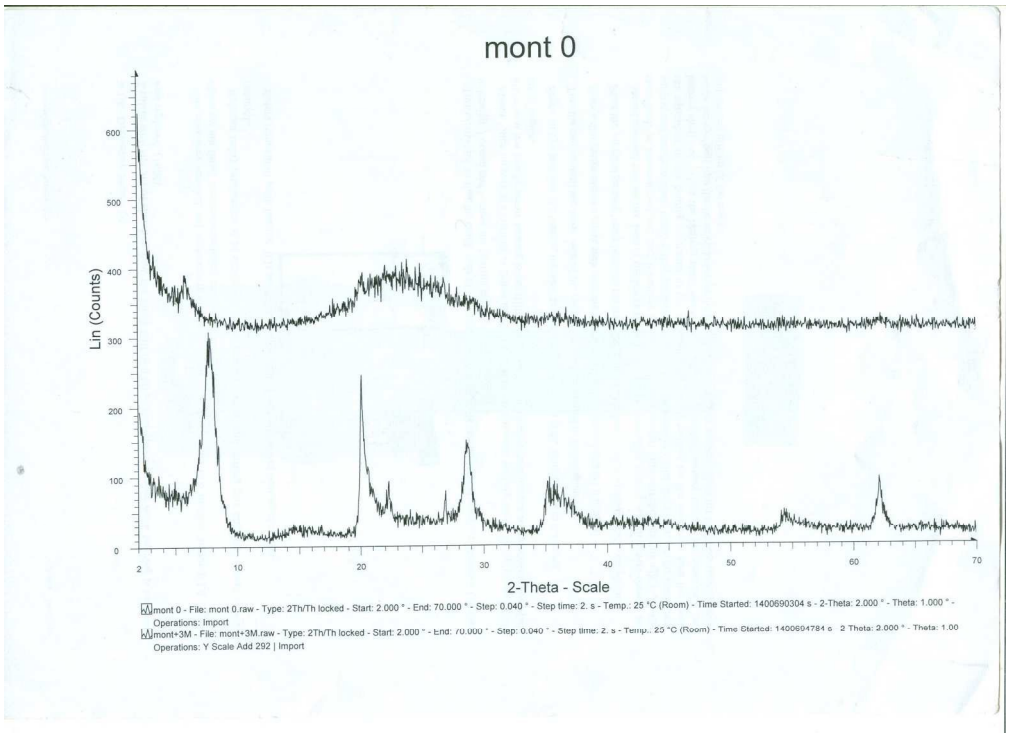

297x215mm (200 x 200 DPI)

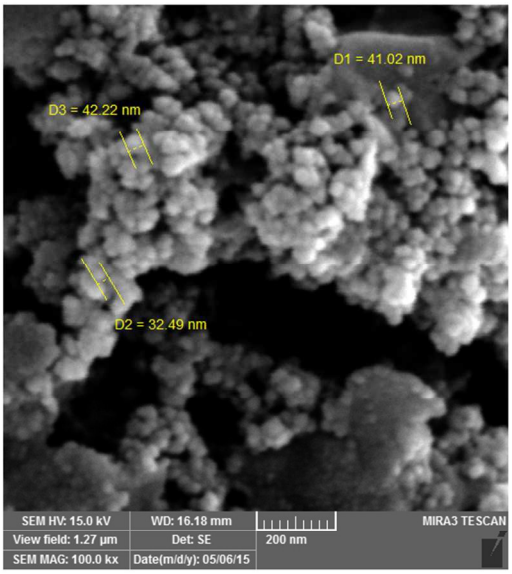

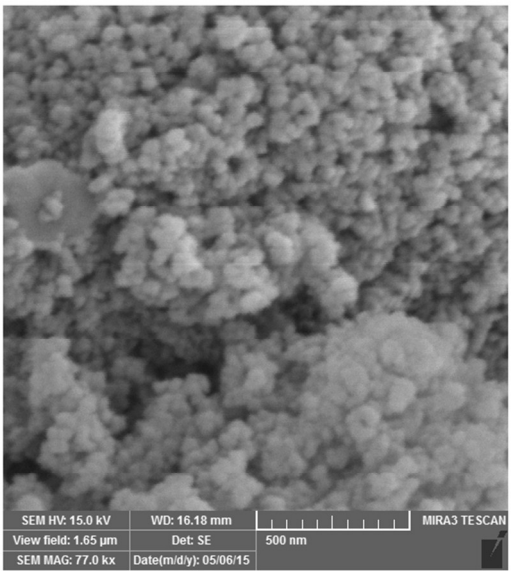

207x321mm (96 x 96 DPI)

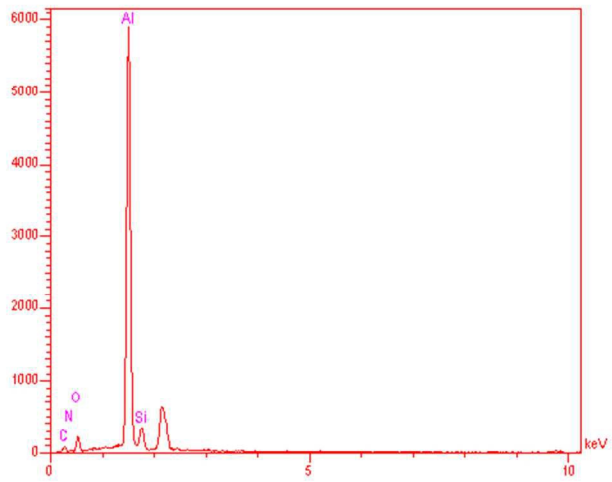

Elt	Line	Int	Error	K	Kr	W%	A%	ZAF	Formula	Ox%	Pk/Bg	Class	LConf	HConf	Cat#
C	Ka	67.3	5.4161	0.0427	0.0255	22.40	36.36	0.1140		0.00	17.65	A	20.68	24.12	0.00
N	Ka	8.2	5.4161	0.0067	0.0040	2.70	3.75	0.1485		0.00	6.55	A	2.10	3.29	0.00
O	Ka	151.2	5.4161	0.0551	0.0329	12.02	14.65	0.2738		0.00	11.86	A	11.41	12.64	0.00
Al	Ka	5010.3	33.5228	0.8327	0.4974	56.57	40.86	0.8793		0.00	102.75	A	56.06	57.07	0.00
Si	Ka	357.5	33.5228	0.0628	0.0375	6.31	4.38	0.5944		0.00	11.95	A	6.10	6.52	0.00
				1.0000	0.5974	100.00	100.00			0.00					0.00

207x171mm (96 x 96 DPI)

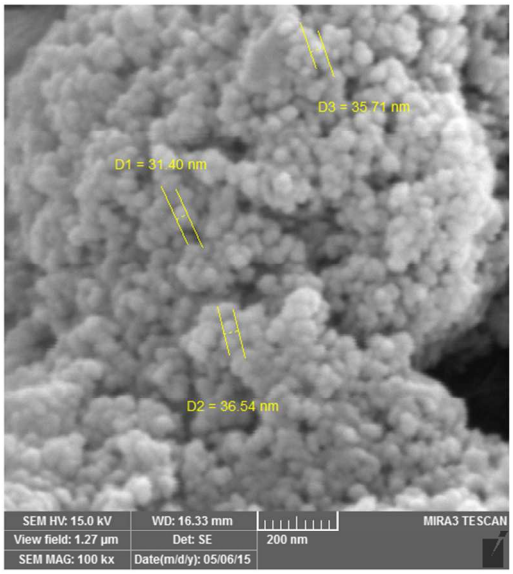

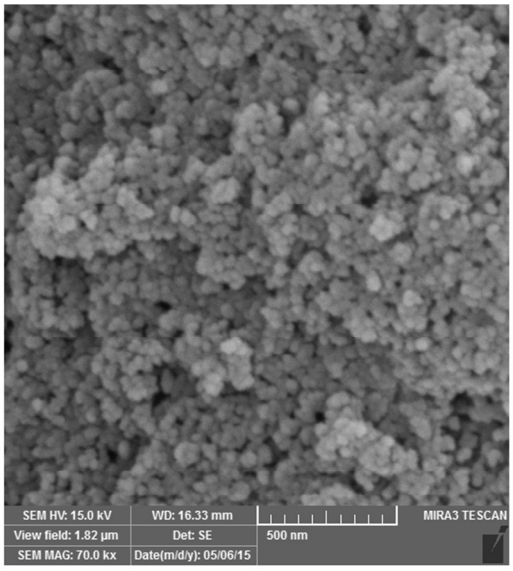

207x321mm (96 x 96 DPI)

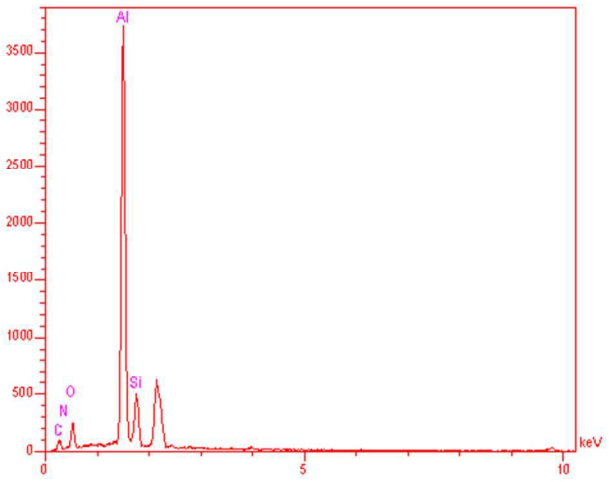

Elt	Line	Int	Error	K	Kr	W%	A%	ZAF	Formula	Ox%	Pk/Bg	Class	LConf	HConf	Cat#
C	Ka	78.7	3.6728	0.0673	0.0337	25.22	38.07	0.1334		0.00	32.59	A	23.43	27.02	0.00
N	Ka	18.8	3.6728	0.0207	0.0104	6.78	8.78	0.1529		0.00	3.46	B	5.79	7.77	0.00
O	Ka	173.6	3.6728	0.0853	0.0427	16.70	18.93	0.2553		0.00	15.20	A	15.90	17.50	0.00
Al	Ka	3170.3	18.5435	0.7099	0.3552	42.19	28.35	0.8418		0.00	82.26	A	41.72	42.66	0.00
Si	Ka	493.7	18.5435	0.1168	0.0584	9.11	5.88	0.6418		0.00	19.94	A	8.85	9.36	0.00
				1.0000	0.5003	100.00	100.00			0.00					0.00

207x171mm (96 x 96 DPI)

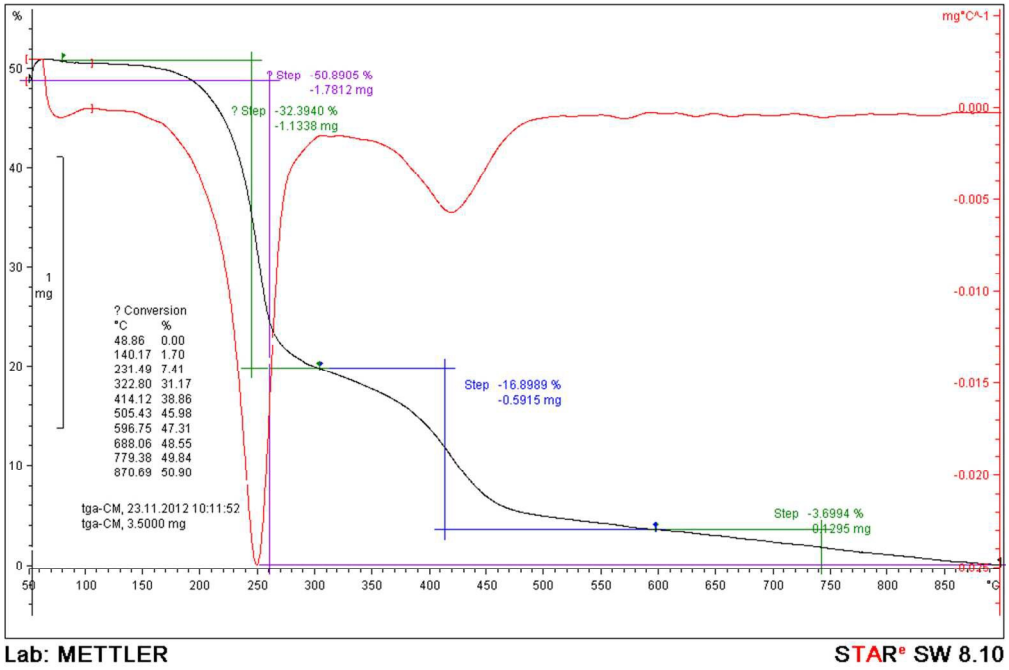

352x243mm (72 x 72 DPI)

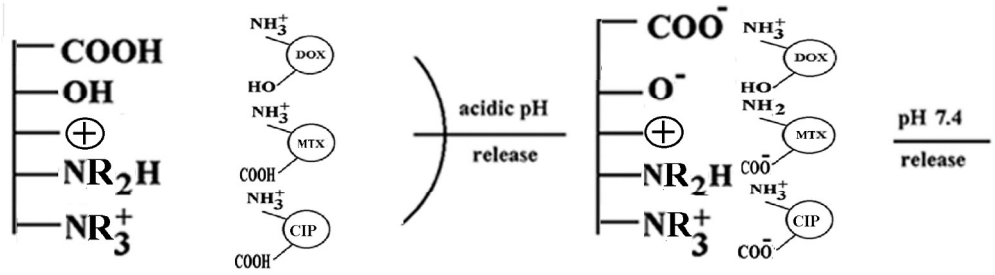

587x166mm (96 x 96 DPI)

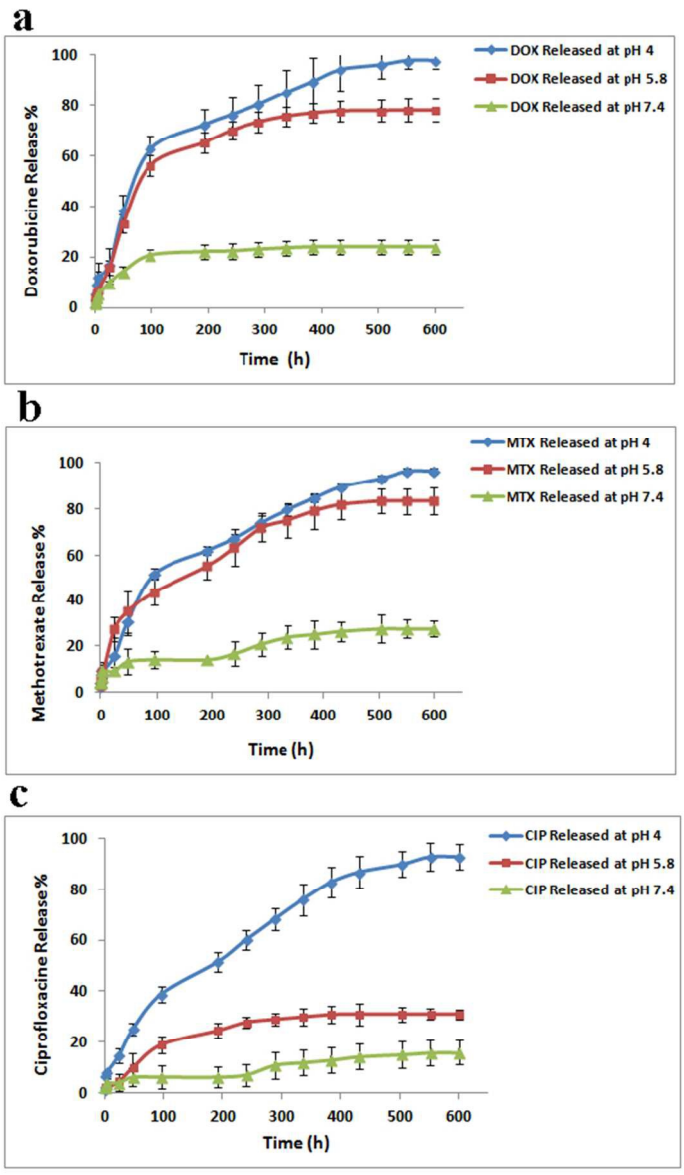

151x260mm (96 x 96 DPI)

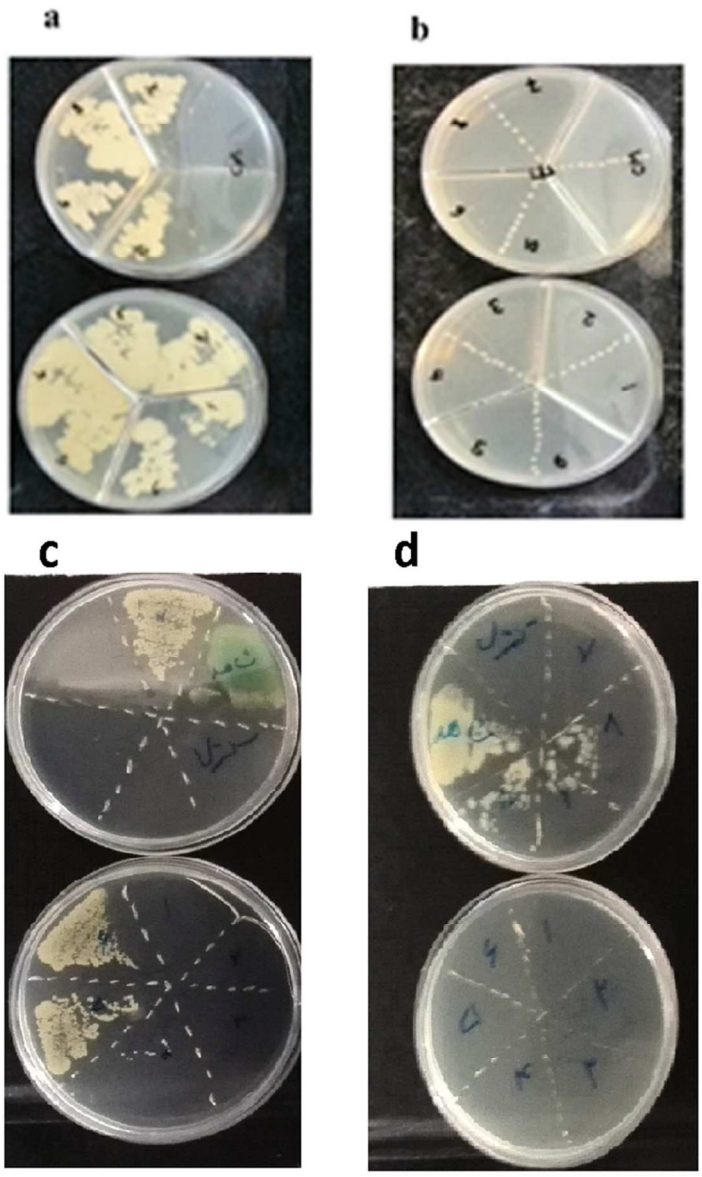

80x124mm (300 x 300 DPI)

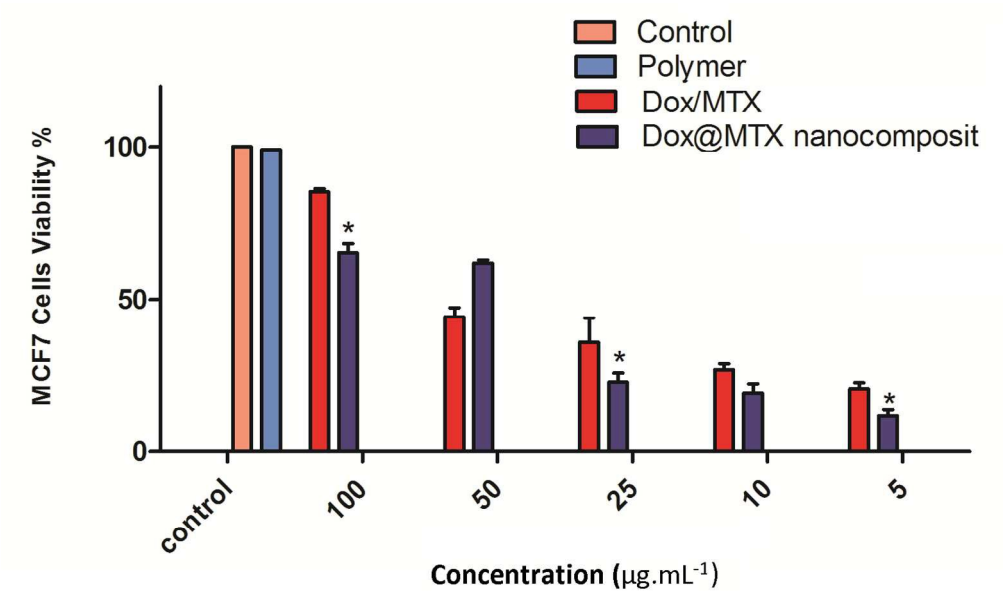

434x273mm (96 x 96 DPI)

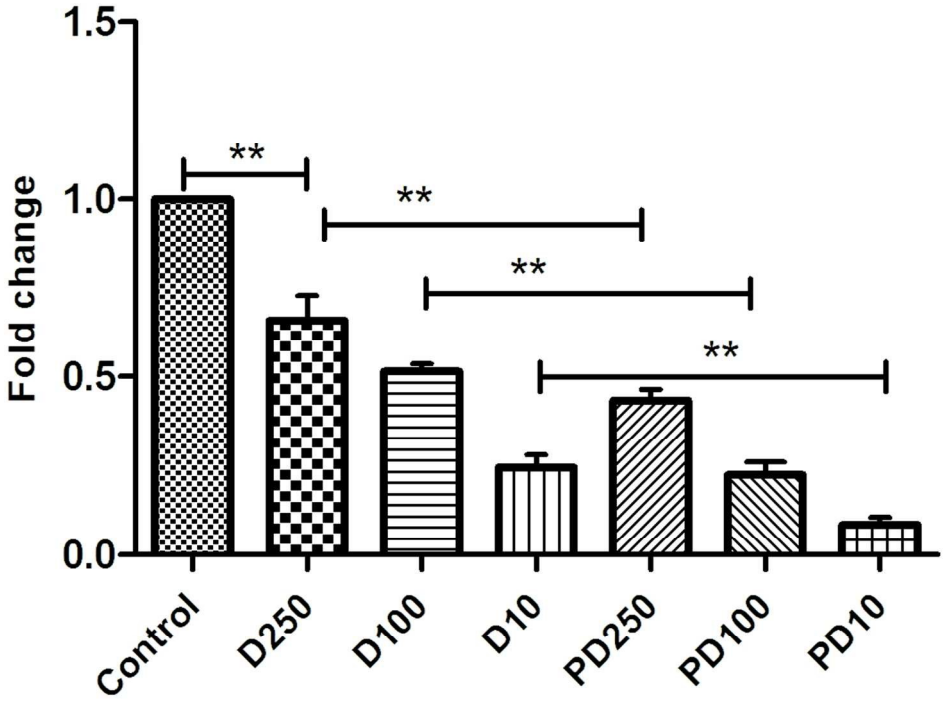

95x75mm (300 x 300 DPI)

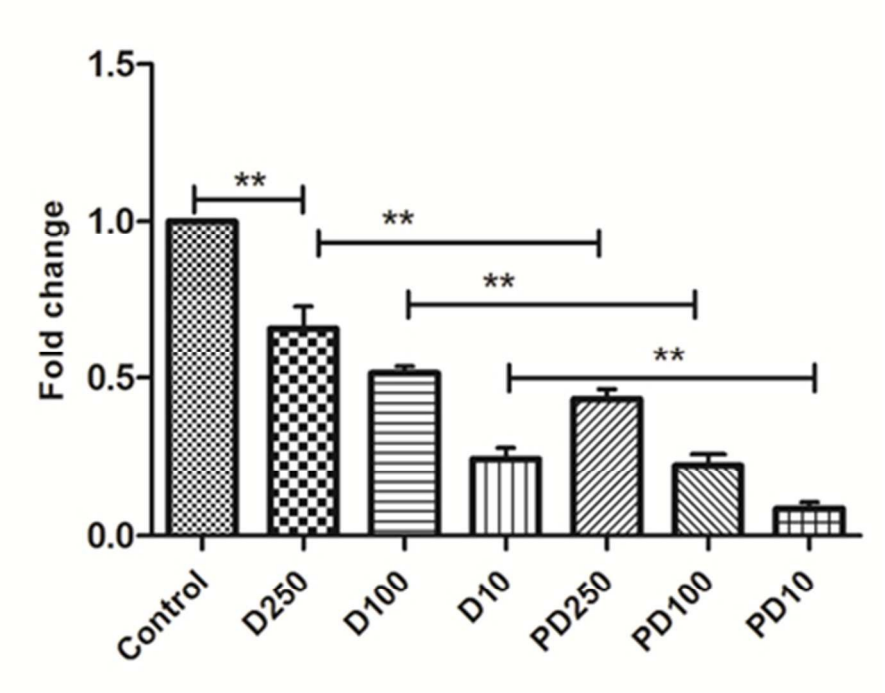

The modified cationic silica based stimuli responsive polymer-clay nanocomposite with pH responsive release manner could improve the targeting performance.

37x39mm (300 x 300 DPI)